

SEP 15 2006

REPORT DOCUMENTATION PAGE			Form Approved OMB No. 0704-0188		
Public reporting burden for this collection of information is estimated to average 1 hour per response, including the time for reviewing instructions, searching existing data sources, gathering and maintaining the data needed, and completing and reviewing the collection of information. Send comments regarding this burden estimate or any other aspect of this collection of information, including suggestions for reducing this burden, to Washington Headquarters Services, Directorate for Information Operations and Reports, 1215 Jefferson Davis Highway, Suite 1204, Arlington, VA 22202-4302, and to the Office of Management and Budget, Paperwork Reduction Project (0704-0188), Washington, DC 20503.					
1. AGENCY USE ONLY (Leave blank)		2. REPORT DATE 17.Aug.06	3. REPORT TYPE AND DATES COVERED MAJOR REPORT		
4. TITLE AND SUBTITLE NONLINEAR SYMPLECTIC ATTITUDE ESTIMATION FOR SMALL SATELLITES.			5. FUNDING NUMBERS		
6. AUTHOR(S) 1ST LT VALPIANI JAMES M					
7. PERFORMING ORGANIZATION NAME(S) AND ADDRESS(ES) UNIVERSITY OF SURREY			8. PERFORMING ORGANIZATION REPORT NUMBER CI04-1880		
9. SPONSORING/MONITORING AGENCY NAME(S) AND ADDRESS(ES) THE DEPARTMENT OF THE AIR FORCE AFIT/CIA, BLDG 125 2950 P STREET WPAFB OH 45433			10. SPONSORING/MONITORING AGENCY REPORT NUMBER		
11. SUPPLEMENTARY NOTES					
12a. DISTRIBUTION AVAILABILITY STATEMENT Unlimited distribution In Accordance With AFI 35-205/AFIT Sup 1			12b. DISTRIBUTION CODE		
13. ABSTRACT (Maximum 200 words)					
14. SUBJECT TERMS			15. NUMBER OF PAGES 16		
			16. PRICE CODE		
17. SECURITY CLASSIFICATION OF REPORT	18. SECURITY CLASSIFICATION OF THIS PAGE	19. SECURITY CLASSIFICATION OF ABSTRACT	20. LIMITATION OF ABSTRACT		

Nonlinear Symplectic Attitude Estimation for Small Satellites

James M. Valpiani*[†] and Philip L. Palmer[‡]

Surrey Space Centre, Guildford, Surrey, GU2 7XH, England

A novel method for efficient high-accuracy satellite attitude estimation is presented to address the increasing performance requirements of resource-constrained small satellites. Symplectic numerical methods are applied to the nonlinear estimation problem for Hamiltonian systems, leading to a new general solution that exactly preserves state probability density functions and conserves invariant properties of the dynamics when solving for the state estimate. This nonlinear Symplectic Filter is applied to a standard small satellite mission and simulation results demonstrate orders of magnitude improvement in state and constants of motion estimation when compared to extended and iterative Kalman methods, particularly in the presence of nonlinear dynamics and high accuracy attitude observations. Based on numerous simulations, the authors conclude that this new method shows promise for improved attitude estimation onboard high performance, resource-constrained small satellites.

I. Introduction

ACCURATE Attitude Determination and Control Subsystem (ADCS) algorithms are crucial for successful satellite operations. This is particularly true for small satellites, where maturing customer needs and broadening mission profiles have led to increasingly stringent precision and performance requirements. Of paramount concern to small satellite ADCS engineering is the ability to autonomously, accurately, and quickly determine orientation in space with minimal expense of onboard resources. The objective of this research is the novel application of symplectic numerical methods to small satellite attitude estimation in order to meet these requirements.

In 1968, Athans et al¹ identified two main methods that were being used to solve the nonlinear filtering problem. The first method approximated the nonlinear dynamical and observation equations in order to utilize linear filtering theory. The second method used approximations to the exact nonlinear filtering solutions such as those found in References 2 and 3. Broadly speaking, estimation solutions continue to fall into one of these two categories.⁴⁻⁶ Primarily because of its low computational burden, the majority of nonlinear estimation methods used on satellites have fallen into the former category, including the ubiquitous Extended Kalman Filter (EKF).^{2,7-9} While this approach has been used extensively, it renders estimation methods poorly-suited for highly nonlinear dynamical systems, leading to an increased demand on satellites to continually update attitude orientation knowledge.¹⁰ On the other hand, approximating optimal nonlinear filtering is particularly difficult since the solution to one of the two governing equations, the Fokker-Planck Equation (also known as the Kolmogorov Forward Equation), is a probability density function extending over an infinite domain. Many efforts have been made to approximate or solve numerically for exact solutions; among these methods are Monte Carlo methods, finite-difference methods, and Fourier series representations, all of which have been documented as computationally expensive or difficult to implement and therefore unsuitable for online implementation.¹¹⁻¹³ The qualities of both these nonlinear estimation methods are troublesome for small satellites with constrained resources and ever-increasing attitude requirements. Recent advancements in small satellite ADCS capabilities such as slewing rates of 3°s^{-1} or better¹⁴ highlight the

*PhD Student, Surrey Space Centre, University of Surrey, Guildford GU2 7XH, England

[†]The views expressed in this article are those of the author and do not reflect the official policy or position of the United States Air Force, Department of Defense, or the U.S. Government.

[‡]Reader, Surrey Space Centre, University of Surrey, Guildford GU2 7XH, England, AIAA Member

20060921208

need for high accuracy efficient attitude estimation methods that can address the shortcomings of both these approaches.

In parallel to these considerations, recent research in the field of estimation has focused on preserving the symplectic properties of Hamiltonian systems.¹⁵⁻¹⁹ In essence, symplecticity indicates that certain global conservation laws apply to a system which take the form of geometric constraints on the space of possible solutions. While the concept of symplecticity is not new, numerical techniques that preserve these values over time are. Compared to other methods, symplectic-preserving numerical methods have demonstrated increased stability and improved long-term performance when applied to Hamiltonian dynamical systems. Consequently, symplectic methods are well suited for accurate long-term propagation and systems where preservation of conserved quantities is important for accurate predictions. Recent research involving symplectic numerical methods has demonstrated promising results when applied to satellite attitude propagation.^{10,20} Additionally, symplectic methods have led to significant improvements in state accuracy and constants of motion accuracy when applied to standard EKF theory for satellite attitude estimation (symplectic EKF, or SKF¹⁷).

This paper presents a novel approach for addressing the shortcomings of the two methods of nonlinear filtering described above by exploiting the strength of the symplectic properties of satellite motion. Because the dynamics of small satellites are well understood, and because disturbances act on long time scales relative to the Hamiltonian motion, initial theory development assumes that unmodeled stochastic accelerations between measurement updates are ignorable. The Fokker-Planck equation which governs the evolution of the state probability density function (pdf) is then reduced to a deterministic problem. In Hamiltonian systems, this leaves the probability density function associated with the system state invariant over time.²¹ Since the resulting deterministic system has symplectic geometry, a symplectic-preserving integrator is used to solve for the evolution of the pdf exactly with the additional benefit of conserving the underlying geometric structure of the motion. The nonlinearly propagated pdf is then combined with a system measurement via Bayes' Rule, and an iterative method is used to determine the state. Once the state has been solved at an update, the standard Kalman Filter covariance update is modified for Hamiltonian systems and applied to the filter in order to create a computationally efficient algorithm. Finally, a form of process noise is reintroduced into the estimation construct in order to increase its robustness to unmodeled disturbances.

In this paper, a new nonlinear solution to the general estimation problem for Hamiltonian systems is presented. First, the equations of motion governing satellite attitude are defined, followed by a brief review of symplecticity and the symplectic attitude propagator used for this research. Then, the nonlinear Symplectic Filter (SF) is derived and applied to the satellite attitude estimation problem. Comparisons with standard estimation techniques demonstrate significantly better performance particularly in the presence of high-accuracy attitude observations and nonlinear dynamics. Finally, conclusions are drawn based on these results.

II. Equations of Motion

Fundamentally, the problem of three-axis attitude parameterization is to specify the orientation of the satellite body frame with respect to another known coordinate frame (commonly, the local orbital or inertial coordinate frames). The equations of satellite motion which govern its orientation are described in this section.

Satellite dynamics in inertial space are governed by Euler's equations of motion. Describing the rotational motion of the satellite with respect to an inertial frame gives

$$\dot{\mathbf{h}} = \mathbf{h} \times (I^{-1}\mathbf{h}) + \mathbf{N} \quad (1)$$

where $\mathbf{h} = I\boldsymbol{\omega}_{b/i}$ is the body angular momentum vector, $I \in \mathbb{R}^{3 \times 3}$ is the moment of inertia tensor of the satellite, $\boldsymbol{\omega}_{b/i} = [\omega_1 \ \omega_2 \ \omega_3]^T$ is the inertially referenced body angular rate vector, $\mathbf{N} \in \mathbb{R}^3$ is the total external torque vector about the satellite center of mass with respect to the inertial coordinate frame, and subscripts 1, 2, and 3 are the axes of the satellite body coordinate frame. In this paper, motion of the satellite is described with respect to principal axes so that the off-diagonal terms of I become zero and the diagonal elements are referred to as I_1 , I_2 , and I_3 .

The orientation of the satellite body between the inertial frame and the body-fixed frame can be represented by Euler parameters, which are expressed here as a 4-vector quaternion $\mathbf{q} \in S^3$. This quaternion is

governed by²²

$$\dot{\mathbf{q}} = \frac{1}{2}\Lambda^T(\mathbf{q})I^{-1}\mathbf{h} \quad (2)$$

where

$$\Lambda = \begin{bmatrix} -q_2 & q_1 & q_4 & -q_3 \\ -q_3 & -q_4 & q_1 & q_2 \\ -q_4 & q_3 & -q_2 & q_1 \end{bmatrix} \quad (3)$$

and \mathbf{q} is subject to

$$\mathbf{q}^T\mathbf{q} = 1 \quad (4)$$

The most significant external torque affecting small satellites is gravity-gradient torque. It is therefore included explicitly in the dynamical model²³

$$\mathbf{N}_{\text{Gravity Gradient}} = \frac{3\mu}{\|\mathbf{r}\|^3} \frac{-\mathbf{r}}{\|\mathbf{r}\|} \times I \frac{-\mathbf{r}}{\|\mathbf{r}\|} \quad (5)$$

where $\|\cdot\|$ is the Euclidean norm, $\mu = GM$ is the Earth's gravitational constant, and \mathbf{r} is the position vector from the center of mass of the Earth to the satellite's center of mass expressed in the orbital frame (defined by a right-handed orthogonal set of axes with its z-axis in the nadir direction and its y-axis in the orbit anti-normal direction). Note that these equations derive from a noncanonical Hamiltonian system that is a Lie-Poisson system with skew-symmetric structure matrix $\mathbf{J}(\mathbf{x})$:²⁴

$$\frac{d}{dt}\mathbf{x} = \mathbf{J}(\mathbf{x})\nabla H(\mathbf{x}) \quad (6)$$

To facilitate later discussion, flow map notation is introduced according to Ref. 21 to describe the solution to Eq. (6). Consider the satellite equations of motion written in general terms

$$\frac{d}{dt}\mathbf{x}_t = f(t, \mathbf{x}_t) \quad (7)$$

with initial state \mathbf{x}_0 . The set of all possible solutions defined by this initial state forms a phase space trajectory, and the flow map $\phi : \mathbb{R}^j \rightarrow \mathbb{R}^j$ defines a mapping between solutions at different times along a given trajectory. The flow map satisfies

$$\frac{d}{dt}\phi = f(t, \phi(t; \mathbf{x}_0, t_0)) \quad (8)$$

$$\phi(t_0; \mathbf{x}_0, t_0) = \mathbf{x}_0 \quad (9)$$

The direct flow map relates an initial state \mathbf{x}_0 at time t_0 to some future state \mathbf{x}_t at time t :

$$\mathbf{x}_t = \phi(t; \mathbf{x}_0, t_0), \quad t \geq t_0 \quad (10)$$

To clarify the direction of time, the inverse flow map is defined to relate an initial state at time t to some previous state at time t_0

$$\mathbf{x}_0 = \psi(t_0; \mathbf{x}_t, t) \quad (11)$$

The two flows are related by the identity

$$\mathbf{x}_0 = \psi(t_0; \phi(t; \mathbf{x}_0, t_0), t) \quad (12)$$

This notation will be used in Section IV to explain the theoretical basis of the nonlinear Symplectic Filter.

III. Symplecticity

The term ‘symplectic’ is associated with a numerical scheme that approximates the solution to a Hamiltonian system while preserving its underlying symplectic structure. More specifically, a symplectic integrator is the exact solution to a discrete perturbed Hamiltonian system that is close to the actual Hamiltonian of interest. Because Hamiltonian systems have volume-preserving mappings in phase space (according to Liouville’s Theorem), symplectic integrators also preserve volume in phase space to within machine precision. Therefore, phase space trajectories do not cross and energy fluctuations about the exact energy are bounded in solutions given by these methods. Practically speaking, symplectic integrators preserve the invariants of motion for Hamiltonian systems to a much higher degree of accuracy than non-symplectic methods of the same order. Generally, non-symplectic methods will introduce secular errors into conserved values of the dynamics over time and therefore misrepresent conservative systems as a dissipative ones.²⁵

A. Integrator

The symplectic integrator used to propagate Eq. (6) for this research is found in Ref. 10. Briefly, it uses the second-order implicit midpoint rule to integrate Euler’s moment equations in conjunction with a second-order leapfrog scheme that governs the order of the kinematics propagation with respect to the dynamics propagation. This composite scheme is based on symmetric methods, making it conceptually simple, stable, and straightforward to implement and to increase in order. Most importantly, it is computationally inexpensive compared to other published symplectic integrators.^{20,26}

The integrator solves Eq. (6) with a few minor modifications. In keeping with standard practice, the propagated quaternion describes the rotation between the body frame and the orbital frame, governed by

$$\dot{\mathbf{q}} = \frac{1}{2} [\Omega(\mathbf{o}_1) - \Omega^*(\mathbf{o}_2)] \mathbf{q} \quad (13)$$

where $\mathbf{o}_1 = [\boldsymbol{\omega}_{b/i}^T \ 0]^T$, $\mathbf{o}_2 = [0 \ n \ 0 \ 0]^T$, n is the orbital mean motion, and

$$\Omega(\mathbf{p}) \mathbf{q} = \begin{bmatrix} p_4 & p_3 & -p_2 & p_1 \\ -p_3 & p_4 & p_1 & p_2 \\ p_2 & -p_1 & p_4 & p_3 \\ -p_1 & -p_2 & -p_3 & p_4 \end{bmatrix} \begin{bmatrix} q_1 \\ q_2 \\ q_3 \\ q_4 \end{bmatrix} = \Omega^*(\mathbf{q}) \mathbf{p} = \begin{bmatrix} q_4 & -q_3 & q_2 & q_1 \\ q_3 & q_4 & -q_1 & q_2 \\ -q_2 & q_1 & q_4 & q_3 \\ -q_1 & -q_2 & -q_3 & q_4 \end{bmatrix} \begin{bmatrix} p_1 \\ p_2 \\ p_3 \\ p_4 \end{bmatrix} \quad (14)$$

The difference between this quaternion and the body to inertial frame quaternion described in Section II is a known rotation, and therefore trivial.

Internal angular momentum changes are associated with active control being applied to a satellite, and to maintain a conservative system the satellite is assumed to be uncontrolled over the course of an individual propagation step. Similarly, external torques are assumed to be zero over the course of a propagation step, which is valid given that the primary torque (gravity gradient) is modeled and that other torques generally operate on timescales much longer than the standard ADCS propagation step. The leapfrog structure of the integrator makes the addition of internal and external torques as impulsive phase space trajectory jumps a straightforward matter.²⁶

The examples in this paper all assume circular Keplerian orbits for simplification, as this eliminates the need to propagate the translational motion variables and reduces the system state to seven variables (four quaternions and three angular rates); however, the estimation method presented below is not restricted to this assumption. While the rigid body motion first integrals of rotational energy and satellite angular momentum measured in the inertial frame are not conserved due to the gravity gradient torque, the circular orbit assumption gives rise to a Jacobi-like integral constant^{10,20}

$$E_J = \frac{1}{2} \sum_k^3 I_k \omega_k^2 + \sqrt{\frac{\mu}{\|\mathbf{r}\|^3}} L_2 + \frac{3\mu}{2\|\mathbf{r}\|^3} \sum_k^3 I_k A_{k3}^2(\mathbf{q}) \quad (15)$$

where $\boldsymbol{\omega} = \boldsymbol{\omega}_{b/i}$ and L_2 is the second component of the angular momentum vector in the inertial frame. This vector is given by

$$\mathbf{L} = D(nt)A(\mathbf{q})^T(\mathbf{h}) \quad (16)$$

where $D(nt) \in SO(3)$ is the rotation matrix from the local orbital frame to the inertial frame and $A(\mathbf{q}) \in SO(3)$ is the quaternion-based rotation matrix from the local orbital frame to the body frame.

In flow map notation, the integrator for this research solves Eq. (6) using a symplectic map ϕ' to approximate the true direct mapping ϕ , and the inverse of the integrator, ψ' , approximates the true inverse mapping ψ .

IV. The Nonlinear Symplectic Filter

A. Theory Development

Fundamentally, estimation is the determination of a system's state in the presence of noisy observations, uncertain initial conditions, and random disturbances too complex to model. This research effort takes the Bayesian approach in solving the estimation problem. Consider the continuous time Itô stochastic differential equation²

$$\frac{d}{dt}\mathbf{x}_t = f(\mathbf{x}_t) + G(\mathbf{x}_t)\boldsymbol{\eta}_t, \quad t \geq t_0 \quad (17)$$

where $\mathbf{x}_t = [x_1 \ x_2 \ \dots \ x_m]^T \in \mathbb{R}^m$ is the system state at time t , $f(\mathbf{x}_t) \in \mathbb{R}^m$ describes the deterministic behavior of the state, $G(\mathbf{x}_t) \in \mathbb{R}^{m \times k}$ characterizes the diffusion, and $\{\boldsymbol{\eta}_t \in \mathbb{R}^k, t \geq t_0\}$ is a zero mean white Gaussian noise process with $\mathcal{E}\{\boldsymbol{\eta}_t, \boldsymbol{\eta}_{t'}\} = Q(t)\delta(t - t')$. Observations of the system are taken at discrete time instants t_n ,

$$\mathbf{z}_n = h(\mathbf{x}_n) + \mathbf{v}_n; \quad n = 1, 2, \dots; \quad t_0 \leq t_n < t_{n+1} \quad (18)$$

where $\mathbf{z}_n \in \mathbb{R}^r$ is a vector of observations, $h(\mathbf{x}_n) \in \mathbb{R}^r$ relates the system states to the observations, and $\{\mathbf{v}_n \in \mathbb{R}^r, n = 1, \dots\}$ is a white Gaussian noise process with $\mathbf{v}_n \sim N(0, R_n)$. For convenience, the state \mathbf{x} at time t will generally be written as \mathbf{x}_t and at discrete time instants t_n will be written as \mathbf{x}_n ; also, functions of the state are generally functions of time t (or t_n), though for convenience this will not be explicitly stated. It is assumed that the initial state, the process noise, and the observation noise are independent, and that some initial state probability density $\wp(\mathbf{x}_0)$ is known.

The nonlinear estimation problem is to find the state estimates conditioned on the observations. This is accomplished by determining the evolution of the conditional probability density function $\wp(\mathbf{x}_n|Z_n)$, where $Z_n = \{\mathbf{z}_d : t_0 < t_d \leq t_n\}$ and $\wp(\mathbf{x}_0|Z_0) = \wp(\mathbf{x}_0)$. Knowing the conditional density function, descriptive statistics can be used to estimate the state. Between observations at times t_{n-1} and t_n , the conditional density $\wp(\mathbf{x}_t|Z_{n-1})$ satisfies the Fokker-Planck equation (also known as the Kolmogorov's Forward equation)¹²

$$\frac{\partial}{\partial t}\wp = - \sum_{i=1}^m \frac{\partial}{\partial x_i} [\wp f_i] + \frac{1}{2} \sum_{i=1}^m \sum_{j=1}^m \frac{\partial^2}{\partial x_i \partial x_j} \left[\wp [GQG^T]_{ij} \right], \quad t_{n-1} \leq t < t_n \quad (19)$$

where $\wp(\mathbf{x}_t|Z_{n-1})$, $f_i(\mathbf{x}_t)$, $G(\mathbf{x}_t)$, and Q_t were replaced by \wp , f_i , G , and Q , respectively, for simplicity.

Using Eq. (19), some conditional density $\wp(\mathbf{x}_{n-1}|Z_{n-1})$ can be evolved in time up to an observation at time t_n , giving the *a priori* density $\wp(\mathbf{x}_n|Z_{n-1})$. Then, the *a posteriori* conditional density $\wp(\mathbf{x}_n|Z_n)$ can be determined via Bayes' Rule²

$$\wp(\mathbf{x}_n|Z_n) = \frac{\wp(\mathbf{z}_n|\mathbf{x}_n, Z_{n-1})\wp(\mathbf{x}_n|Z_{n-1})}{\wp(\mathbf{z}_n|Z_{n-1})} \quad (20)$$

The *a posteriori* conditional density $\wp(\mathbf{x}_n|Z_n)$ is the complete solution of the nonlinear estimation problem because it embodies all statistical information about \mathbf{x} at t_n which is contained in the observations and the initial condition $\wp(\mathbf{x}_0)$.²

Returning to the system dynamics in Eq. (17), note that Q is used to account for unknown disturbances and process noise by modeling them as stochastic. However, the dynamics for small satellites are well known¹⁰ and for the time being, these unknown disturbances are considered small enough to be ignored. Under this assumption, the Fokker-Planck equation reduces to a deterministic Hamiltonian system, as shown below (note that the following discussion on the Fokker-Planck equation has been adapted from Scheeres and Park²¹)

$$\frac{\partial}{\partial t}\wp = - \sum_{i=1}^m \frac{\partial}{\partial x_i} [\wp f_i] \quad (21)$$

Using the Lie-Poisson system described in Section II,

$$\frac{d}{dt}\mathbf{x} = \mathbf{J}(\mathbf{x})\nabla H(\mathbf{x})$$

then Eq. (21) can be written as

$$\frac{\partial}{\partial t}\wp = - \left[\frac{\partial}{\partial \mathbf{x}} \wp \right]^T \mathbf{f} - \wp \sum_{i=1}^m \frac{\partial}{\partial \mathbf{x}_i} [\mathbf{J}(\mathbf{x})\nabla H(\mathbf{x})]_i \quad (22)$$

Due to the unique structure of Eq. (6) which is a result of the system's Hamiltonian nature, it can be shown that Eq. (22) reduces to

$$\frac{d}{dt}\wp = 0 \quad (23)$$

Using the fundamental theorem of calculus and the integral invariance of the probability of a dynamical system without diffusion, it can be shown that for Hamiltonian systems Eq. (23) gives

$$\wp(\phi(t; \mathbf{x}_0, t_0)) = \wp(\mathbf{x}_0) \left| \frac{\partial \mathbf{x}_t}{\partial \mathbf{x}_0} \right|^{-1} \quad (24)$$

The symplectic nature of the Hamiltonian system implies that²⁷ $\left| \frac{\partial \mathbf{x}_t}{\partial \mathbf{x}_0} \right| = 1$ where $|\cdot|$ is the determinant. Therefore, given an initial state and its associated pdf, the flow map for the Hamiltonian system enables the full characterization of the pdf at any time:

$$\wp(\phi(t; \mathbf{x}_0, t_0)) = \wp(\mathbf{x}_0) \quad (25)$$

$$\wp(\psi(t_0; \mathbf{x}, t)) = \wp(\mathbf{x}_0) \quad (26)$$

For the satellite attitude problem, the true solution flow ϕ is nonlinear and requires the use of a numerical integrator in order to solve for the system state. While symplectic integrators by definition satisfy $\left| \frac{\partial \mathbf{x}_t}{\partial \mathbf{x}_0} \right| = 1$, the most commonly applied integrators such as standard Runge-Kutta methods²⁸ do not preserve the symplectic structure of Hamiltonian systems and therefore do not satisfy the flow condition. For dynamical propagations with relatively noisy observations, this tends not to be a significant concern. In these cases, the observation noise drowns out any differences between numerical methods. However, small satellites are increasingly using high-accuracy position observations in lieu of rate-sensing equipment,²⁹ such as the ESA PROBA-1 mission. Its star camera, the Advanced Stellar Compass (ASC),³⁰ demonstrated arc-second level accuracy and performed at rates of up to $2.5^\circ s^{-1}$. Recent research has demonstrated that, given this combination of nonlinear dynamics and high accuracy observations, the use of a symplectic propagator results in significant accuracy improvements over standard nonsymplectic propagators for state and constants of motion estimation.¹⁷

Considering these results in the context of the nonlinear estimation problem, this means that a probability density function of a deterministic Hamiltonian system can be completely characterized as it transforms forward in time to a level of accuracy limited only by the numerical method employed for state propagation. Using a symplectic method to propagate the density function for the satellite attitude problem preserves the integral invariants of the motion, including state probability and the Jacobi-like constant in Eq. (15). In contrast, approximate nonlinear estimation techniques only propagate a finite amount of information contained in the density function (typically, the mean and covariance) in order to estimate the state. Utilizing the result above, all information contained in a density function (generally composed of an infinite number of moments) can be carried forward in a way that preserves its nonlinearity and the underlying geometric structure of the Hamiltonian system.

B. Symplectic Filter Equations

1. State Estimation

Applying the result from Subsection A to the estimation problem, assume an initial conditional density function at time t_n

$$\wp(\mathbf{x}_n | Z_n) \quad (27)$$

Equation (25) gives the evolution of this initial conditional density function between observations. Therefore, at the next observation time t_{n+1} , the transformed density function is

$$\wp(\mathbf{x}_{n+1}|Z_n) = \wp(\psi'(t_n; \mathbf{x}_{n+1}, t_{n+1})|Z_n) \quad (28)$$

Given this *a priori* density function, the new observation \mathbf{z}_{n+1} , and its density function, Bayes' rule can be used to determine the *a posteriori* density function $\wp(\mathbf{x}_{n+1}|Z_{n+1})$.

At this point, no assumptions have been made about the types of density functions used; to realize an actual filter, these functions must be defined. Assume that the initial state density $\wp(\mathbf{x}_n|Z_n)$ is Gaussian. Assume also that observations have additive white Gaussian noise as in Eq. (18) so that the observation density $\wp(\mathbf{z}_{n+1}|\mathbf{x}_{n+1}, Z_n) = \wp(\mathbf{z}_{n+1}|\mathbf{x}_{n+1})$. Using Bayes' Rule from Eq. (20)

$$\wp(\mathbf{x}_{n+1}|Z_{n+1}) = ce^{-\frac{1}{2}(\cdot)} \quad (29)$$

$$(\cdot) = [\psi'(t_n; \mathbf{x}_{n+1}, t_{n+1}) - \hat{\mathbf{x}}_n]^T \hat{P}_n^{-1} [\psi'(t_n; \mathbf{x}_{n+1}, t_{n+1}) - \hat{\mathbf{x}}_n] + [\mathbf{z}_{n+1} - h(\mathbf{x}_{n+1})]^T R_{n+1}^{-1} [\mathbf{z}_{n+1} - h(\mathbf{x}_{n+1})] \quad (30)$$

where $\hat{\mathbf{x}}_n$ is the state estimate and \hat{P}_n is the covariance estimate at time t_n . Note that the constant

$$c = \frac{1}{\int \wp(\mathbf{z}_{n+1}|\xi, t_{n+1}) \wp(\xi, t_{n+1}|Z_n) d\xi} \quad (31)$$

is independent of \mathbf{x} , and that the normalizing constants $\frac{1}{|2\pi R_{n+1}|^{\frac{1}{2}}}$ in $\wp(\mathbf{z}_{n+1}|\mathbf{x}_{n+1})$ and $\frac{1}{|2\pi \hat{P}_n|^{\frac{1}{2}}}$ in $\wp(\mathbf{x}_n|Z_n)$ are independent of \mathbf{x} and therefore cancel between the numerator and denominator when applying Eq. (20).

The density $\wp(\mathbf{x}_{n+1}|Z_{n+1})$ is the full solution to the nonlinear estimation problem, and its mean is commonly used as the state estimate. However, because of the constraint imposed by the nonlinear inverse flow map in Eq. (29), $\wp(\mathbf{x}_{n+1}|Z_{n+1})$ is generally not a Gaussian density function and determining its mean is nontrivial. Most methods used to do so are prohibitively computationally expensive as discussed in Section I. If $\wp(\mathbf{x}_{n+1}|Z_{n+1})$ is unimodal and concentrated about the mean, then there is a negligible difference between the mean and the mode (or peak) of the density function.⁴ In fact, Bell and Cathey proved that the EKF is simply the first Gauss-Newton iterate in solving for the mode of the *a posteriori* density function, and that the Iterated Extended Kalman Filter (IEKF) uses multiple Gauss-Newton iterates to solve for the mode.^{2,4,31} In addition to being the maximum likelihood estimator, the mode represents a possible system state whereas the mean is not always guaranteed to do so. In the case of quaternions, the means of each of the quaternion components in a distribution do not generally compose a unit quaternion.³² For these reasons, the mode is used as the state estimate for this filter.

Determining the mode of the *a posteriori* density function is equivalent to finding the maximum of Eq. (29). Since the maximum of $\wp(\mathbf{x}_{n+1}|Z_{n+1})$ is the maximum of any monotonic function of $\wp(\mathbf{x}_{n+1}|Z_{n+1})$, and since the natural logarithm is monotonic, then the mode of the pdf can be stated as⁴

$$\hat{\mathbf{x}}_{n+1} = \arg \min_{\mathbf{x}_{n+1}} (\cdot) \quad (32)$$

where (\cdot) is defined in Eq. (30). This problem can be reformulated in to a nonlinear least squares problem

$$\hat{\mathbf{x}}_{n+1} = \arg \min_{\mathbf{x}_{n+1}} \Psi^T(\mathbf{x}_{n+1})\Psi(\mathbf{x}_{n+1}) \quad (33)$$

where

$$\Psi(\mathbf{x}_{n+1}) = S_{n+1}^{-\frac{1}{2}} V(\mathbf{x}_{n+1}) \quad (34)$$

$$S_{n+1} = \begin{bmatrix} P_n & 0 \\ 0 & R_{n+1} \end{bmatrix} \quad (35)$$

$$V(\mathbf{x}_{n+1}) = \begin{bmatrix} \psi'(t_n; \mathbf{x}_{n+1}, t_{n+1}) \\ \mathbf{z}_{n+1} \end{bmatrix} - \begin{bmatrix} \hat{\mathbf{x}}_n \\ h(\mathbf{x}_{n+1}) \end{bmatrix} \quad (36)$$

and $\left[S_{n+1}^{\frac{1}{2}}\right]^T S_{n+1}^{\frac{1}{2}} = S_{n+1}$. In addition to the least squares formulation, a constraint must be added to preserve the quaternion norm $\|\mathbf{q}\| = 1$. A number of methods exist for iteratively solving this problem.³³ For this research, the Levenberg-Marquardt algorithm was implemented due to its robustness and global convergence properties.

Once the mode has been found, the nonlinear estimation problem is essentially solved. However, the issue of recursion remains unaddressed. From Eq. (29), the obvious difficulty for recursion is in preserving the inverse flow map dependency of the *a priori* pdf. It is possible to preserve this dependency completely such that the solution to the nonlinear estimation problem at any future time $t \geq t_0$ would require a backward propagation to the initial time t_0 . This approach would require the preservation of all measurement values up to and including \mathbf{z}_t . However, the computational expense and storage burden would rapidly accumulate, rendering the filter inefficient and running the risk of placing too much confidence in the original pdf, which is often nothing more than an educated guess. Therefore, to ensure an efficient algorithm, the iterative nonlinear least squares method described above is coupled with linear error propagation theory which has been modified for Hamiltonian systems.

2. Error Covariance Propagation

The deviation between a deterministic reference trajectory with state \mathbf{x} and a nonlinear system model with state $\bar{\mathbf{x}}$ can be described by a linearized stochastic system²

$$\frac{d}{dt} \delta \mathbf{x}_t = \left[\frac{\partial}{\partial \mathbf{x}_t} f(\mathbf{x}_t) \right] \delta \mathbf{x}_t \quad (37)$$

where $\delta \mathbf{x}_t \in \mathbb{R}^m = \bar{\mathbf{x}}_t - \mathbf{x}_t$ is state deviation at time t , $f(\mathbf{x}_t) \in \mathbb{R}^m$ describes the deterministic behavior of the system state, and $\delta \mathbf{x}_0 \sim N(\hat{\mathbf{x}}_0 - \hat{\mathbf{x}}_0, P_0)$. This equation can be discretized as

$$\delta \mathbf{x}_{n+1} = \Phi(\mathbf{x}_{n+1}, \mathbf{x}_n) \delta \mathbf{x}_n \quad (38)$$

where

$$\Phi(\mathbf{x}_{n+1}, \mathbf{x}_n) = \frac{\partial \mathbf{x}_{n+1}}{\partial \mathbf{x}_n} \quad (39)$$

$\Phi \in \mathbb{R}^{m \times m}$ is the state transition matrix used in linear systems theory and the EKF. Using the Darboux-Weinstein theorem,³⁴ it can be shown that this linearized Hamiltonian system is itself Hamiltonian. This motivates the application of symplectic methods to the linearized equations in order to preserve the underlying geometric structure of the system. Given the symplectic flow map ϕ' for the satellite attitude problem described in Section III,

$$\frac{\partial}{\partial \mathbf{x}} \phi'(t_{n+1}; \mathbf{x}_n, t_n) = \quad (40)$$

$$\left. \frac{\partial}{\partial \mathbf{x}} \phi'(t_n + \Delta t; \mathbf{x}, t_n) \right|_{\mathbf{x}_{t_n}} \left. \frac{\partial}{\partial \mathbf{x}} \phi'(t_n + 2\Delta t; \mathbf{x}, t_n + \Delta t) \right|_{\mathbf{x}_{t_n + \Delta t}} \cdots \left. \frac{\partial}{\partial \mathbf{x}} \phi'(t_{n+1}; \mathbf{x}, t_n + (j-1)\Delta t) \right|_{\mathbf{x}_{t_n + (j-1)\Delta t}} \quad (41)$$

where $t_{n+1} = t_n + j\Delta t$. From the definition of a flow map in Eq. (10), it is clear that

$$\frac{\partial}{\partial \mathbf{x}} \phi'(t_{n+1}; \mathbf{x}_n, t_n) = \prod_{m=0}^{j-1} \frac{\partial \mathbf{x}_{t_n + (m+1)\Delta t}}{\partial \mathbf{x}_{t_n + m\Delta t}} = \frac{\partial \mathbf{x}_{n+1}}{\partial \mathbf{x}_n} \quad (42)$$

This describes a flow map which is also symplectic and therefore preserves the linearized Hamiltonian system in Eq. (38). The symplecticity of the flow map can be demonstrated straightforwardly if

$$\left| \frac{\partial}{\partial \mathbf{x}} \phi'(t_{n+1}; \mathbf{x}_n, t_n) \right| = 1 \quad (43)$$

However, as previously discussed, the condition $\left| \frac{\partial \mathbf{x}_{n+1}}{\partial \mathbf{x}_n} \right| = 1$ is true for all symplectic numerical methods. Thus, Eq. (42) shows that $\frac{\partial}{\partial \mathbf{x}} \phi'(t_{n+1}; \mathbf{x}_n, t_n)$ is symplectic.

Returning to the definition of the state transition matrix in Eq. (39), it is clear that Φ preserves the linearized Hamiltonian structure of Eq. (38). This is particularly useful since the components of Φ are already calculated for the nonlinear least squares method to determine the state estimate. Once the state estimate $\hat{\mathbf{x}}_{n+1}$ is known at time t_{n+1} , the SF propagates the error covariance matrix estimate \hat{P}_n from time t_n using standard Kalman Filter equations

$$P_{n+1} = \Phi(\hat{\mathbf{x}}_{n+1}, \bar{\mathbf{x}}_n) \hat{P}_n \Phi^T(\hat{\mathbf{x}}_{n+1}, \bar{\mathbf{x}}_n) \quad (44)$$

modified such that

$$\Phi(\hat{\mathbf{x}}_{n+1}, \bar{\mathbf{x}}_n) = \frac{\partial}{\partial \mathbf{x}} \phi'(t_{n+1}; \bar{\mathbf{x}}_n, t_n) \quad (45)$$

where

$$\bar{\mathbf{x}}_n = \psi'(t_n; \hat{\mathbf{x}}_{n+1}, t_{n+1}) \quad (46)$$

Note that, in general, the state estimate $\hat{\mathbf{x}}_{n+1} \neq \phi'(t_{n+1}; \hat{\mathbf{x}}_n, t_n)$, and therefore the notation $\bar{\mathbf{x}}_n$ has been introduced to indicate the initial state at time t_n that maps to the state estimate $\hat{\mathbf{x}}_{n+1}$ at time t_{n+1} . Once P_{n+1} is known, it is used to approximate the *a priori* pdf via a Gaussian distribution. Finally, the standard Kalman Filter equations are used to approximate the Gaussian *a posteriori* pdf and its covariance matrix, \hat{P}_{n+1} .

This approach is distinct from the standard EKF in that it exactly conserves the underlying geometry of the linearized Hamiltonian system. Practically speaking, the symplecticity of Hamiltonian systems implies the preservation of the volume of phase space subsets; in other words, the volume defined by a set of system solutions in phase space at any given time will remain constant for all time. Therefore, the Hamiltonian nature of satellite attitude motion demands that the volumes defined by the level sets of the initial state pdf remain constant throughout the evolution of the pdf. For a deterministic Hamiltonian system with an initial Gaussian pdf and linearized dynamics, this requirement is equivalent to preserving the volume of the ellipsoid defined by the error covariance matrix; this is clearly satisfied by the state transition matrix Φ and its unity determinant.

3. Process Noise

The final unresolved matter for SF implementation is the reintroduction of stochastic accelerations and process noise. In the standard Kalman Filter, these are accounted for in the Q matrix which is generally assumed to be additive Gaussian noise with covariance matrix²

$$Q_{n+1} = \int_0^{\Delta t} \Phi(t_{n+1}, t_n + \tau) G(t_n + \tau) Q(t_n + \tau) G^T(t_n + \tau) \Phi^T(t_{n+1}, t_n + \tau) d\tau \quad (47)$$

where $\Delta t = t_{n+1} - t_n$, $G(t_n + \tau)$ relates the zero-mean white noise process defined by $Q(t_n + \tau)$ to the state, and the state has been temporarily omitted from the notation to emphasize dependency on time (see Eq. (17) for the definitions of Q and G in the dynamical equations). In each iteration of the Kalman Filter, the process noise covariance matrix Q_{n+1} is added to the propagated error covariance matrix to determine the predicted error covariance

$$P_{n+1} = \Phi(t_{n+1}, t_n) \hat{P}_n \Phi^T(t_{n+1}, t_n) + Q_{n+1} \quad (48)$$

This approach will generally not work for the SF, which does not propagate the error covariance matrix until after the state estimate has been determined. Instead, the SF solves for the covariance matrix \tilde{Q}_n that, when added to \hat{P}_n , leads to the error covariance matrix in Eq. (48):

$$\Phi(t_{n+1}, t_n) [\hat{P}_n + \tilde{Q}_n] \Phi^T(t_{n+1}, t_n) = \Phi(t_{n+1}, t_n) \hat{P}_n \Phi^T(t_{n+1}, t_n) + Q_{n+1} \quad (49)$$

This readily reduces to

$$\tilde{Q}_n = \Phi^{-1}(t_{n+1}, t_n) Q_{n+1} (\Phi^T)^{-1}(t_{n+1}, t_n) \quad (50)$$

Note that this approach assumes the state transition matrix is a good approximation to the true nonlinear flow. This is justified in part because of the SF's theoretically accurate state transition matrix $\Phi(t_{n+1}, t_n)$. Though this is a first-order approximation, it is nevertheless acceptable considering that process noise is treated as a tuning factor in filter implementation, therefore requiring less rigorous treatment.

. Since Φ is known to a high degree of accuracy in the SF, a solution for \tilde{Q}_n based on Φ is ideal. Begin with an alternative definition of Φ ,

$$\frac{d\Phi(t, \tau)}{dt} = F(t)\Phi(t, \tau) \quad (51)$$

where

$$F(t) = \left[\frac{\partial}{\partial \mathbf{x}} f(\mathbf{x}) \right] \Big|_{\mathbf{x}_t} \quad (52)$$

is the matrix of partial derivatives of the state evaluated at t . The solution is a matrix exponential

$$\Phi(t, \tau) = e^{\int_{\tau}^t F(s) ds} \quad (53)$$

The Taylor expansion of the matrix exponential gives

$$\Phi(t, \tau) = \mathbf{I} + \int_{\tau}^t F(s) ds + \text{H.O.T.} \quad (54)$$

Ignoring higher order terms (H.O.T) and applying Euler's method to the integral gives

$$\Phi(t, \tau) = \mathbf{I} + F(t)(t - \tau) \quad (55)$$

Assuming stochastic errors in the angular rates only, define $G = [0_{3 \times 4} \quad \mathbf{I}_3]^T$ and

$$Q = \begin{pmatrix} \sigma_1 & 0 & 0 \\ 0 & \sigma_2 & 0 \\ 0 & 0 & \sigma_3 \end{pmatrix} \quad (56)$$

such that

$$\Upsilon = GQG^T = \begin{bmatrix} 0 & 0 \\ 0 & Q \end{bmatrix} \quad (57)$$

where $\Upsilon \in \mathbb{R}^{7 \times 7}$. Substituting these results into Eqn. (47) gives

$$Q_{n+1} = \int_0^{\Delta t} (\mathbf{I} + F(t_{n+1})(t_{n+1} - (t_n + \tau))) \Upsilon (\mathbf{I} + F^T(t_{n+1})(t_{n+1} - (t_n + \tau))) d\tau \quad (58)$$

This integral evaluates to

$$Q_{n+1} = \Psi \Delta t + \Upsilon F^T(t_{n+1}) \frac{\Delta t^2}{2} + F(t_{n+1}) \Upsilon \frac{\Delta t^2}{2} + F(t_{n+1}) \Upsilon F^T(t_{n+1}) \frac{\Delta t^3}{3} \quad (59)$$

Rearranging Eqn. (55),

$$F(t_{n+1}) = \frac{\Phi(t_{n+1}, t_n) - \mathbf{I}}{\Delta t} \quad (60)$$

Substituting this definition into Eqn. (59), omitting time notation for convenience, and simplifying gives

$$Q_{n+1} = \frac{\Delta t}{6} (\Phi \Upsilon + \Upsilon \Phi^T + 2\Phi \Upsilon \Phi^T + 2\Upsilon) \quad (61)$$

Finally, applying this result to Eqn. (50) and simplifying gives

$$\tilde{Q}_n = \frac{\Delta t}{6} (\chi \Gamma + \Gamma^T \chi^T + 2\Upsilon) \quad (62)$$

where $\chi = \mathbf{I} + \Phi^{-1}$ and $\Gamma = \Upsilon(\Phi^{-1})^T$. When applied in the SF, Φ is defined by Eq. (45) in order to conserve the linearized Hamiltonian. In theory, \tilde{Q}_n should be recalculated at every iteration of the Levenberg-Marquardt algorithm. However, many experiments with the SF have shown that this approach leads to negligible performance gain. Therefore, in order to minimize computational expense, \tilde{Q}_n is calculated once per iteration.

C. Summary

The nonlinear Symplectic Filter is summarized below. Assuming an initial state $\hat{\mathbf{x}}_n$, initial error covariance matrix \hat{P}_n , process noise matrix Q , and system observations \mathbf{z} with covariance R , the SF is governed by the following equations:

Initial Calculations

$$\Upsilon = \begin{bmatrix} 0 & 0 \\ 0 & Q \end{bmatrix} \quad (63)$$

State Prediction

$$\bar{\mathbf{x}}_{n+1} = \phi'(t_{n+1}; \hat{\mathbf{x}}_n, t_n) \quad (64)$$

$$\bar{\Phi}(\bar{\mathbf{x}}_{n+1}, \hat{\mathbf{x}}_n) = \frac{\partial}{\partial \mathbf{x}} \phi'(t_{n+1}; \hat{\mathbf{x}}_n, t_n) \quad (65)$$

$$\chi_n = \mathbf{I} + \bar{\Phi}^{-1}(\bar{\mathbf{x}}_{n+1}, \hat{\mathbf{x}}_n) \quad (66)$$

$$\Gamma_n = \Upsilon(\bar{\Phi}^{-1})^T(\bar{\mathbf{x}}_{n+1}, \hat{\mathbf{x}}_n) \quad (67)$$

$$\bar{Q}_n = \frac{\Delta t}{6}(\chi_n \Gamma_n + \Gamma_n^T \chi_n^T + 2\Upsilon) \quad (68)$$

State Estimation

$$S_{n+1} = \begin{bmatrix} \hat{P}_n + \bar{Q}_n & 0 \\ 0 & R_{n+1} \end{bmatrix} \quad (69)$$

$$V(\mathbf{x}_{n+1}) = \begin{bmatrix} \psi'(t_n; \mathbf{x}_{n+1}, t_{n+1}) \\ \mathbf{z}_{n+1} \end{bmatrix} - \begin{bmatrix} \hat{\mathbf{x}}_n \\ h(\mathbf{x}_{n+1}) \end{bmatrix} \quad (70)$$

$$\Psi(\mathbf{x}_{n+1}) = S_{n+1}^{-\frac{1}{2}} V(\mathbf{x}_{n+1}) \quad (71)$$

$$\hat{\mathbf{x}}_{n+1} = \arg \min_{\mathbf{x}_{n+1}} \Psi^T(\mathbf{x}_{n+1}) \Psi(\mathbf{x}_{n+1}) \quad (72)$$

Error Covariance Propagation

$$\bar{\mathbf{x}}_n = \psi'(t_n; \hat{\mathbf{x}}_{n+1}, t_{n+1}) \quad (73)$$

$$\hat{\Phi}(\hat{\mathbf{x}}_{n+1}, \bar{\mathbf{x}}_n) = \frac{\partial \hat{\mathbf{x}}_{n+1}}{\partial \bar{\mathbf{x}}_n} \quad (74)$$

$$H_{n+1} = \left[\frac{\partial}{\partial \mathbf{x}} h(\mathbf{x}) \right] \Big|_{\bar{\mathbf{x}}_{n+1}} \quad (75)$$

$$\bar{P}_{n+1} = \hat{\Phi}(\hat{\mathbf{x}}_{n+1}, \bar{\mathbf{x}}_n) (\hat{P}_n + \bar{Q}_n) \hat{\Phi}^T(\hat{\mathbf{x}}_{n+1}, \bar{\mathbf{x}}_n) \quad (76)$$

$$\hat{P}_{n+1} = \bar{P}_{n+1} - \bar{P}_{n+1} H_{n+1}^T [H_{n+1} \bar{P}_{n+1} H_{n+1}^T + R_{n+1}]^{-1} H_{n+1} \bar{P}_{n+1} \quad (77)$$

To illustrate the merits of the SF over the EKF, consider the examples in figure 1. Given a nonlinear pendulum, assume an uncertainty in the initial conditions in phase space represented by a Gaussian distribution of points (blue). At some future time, the propagated points (red) represent the *a priori* density. The figure on the top right is the EKF approximation which uses linearized dynamics and only calculates the first two moments of the *a priori* density (represented here in a Gaussian distribution). The figure on the top left is the SF approximation which makes no assumption about the form of the *a priori* density when determining the state estimate and accurately transforms the original Gaussian density through the nonlinearity of the system dynamics. Here, the SF approximates the *a priori* density with much greater fidelity than the EKF. Assuming that these probability densities are based on a predicted state that is slightly perturbed from the true state and incorporating a random noisy observation gives the *a posteriori* densities seen in the lower left and right figures. The SF's preservation of density function nonlinearity allows it to estimate the state to a higher degree of accuracy than the EKF.

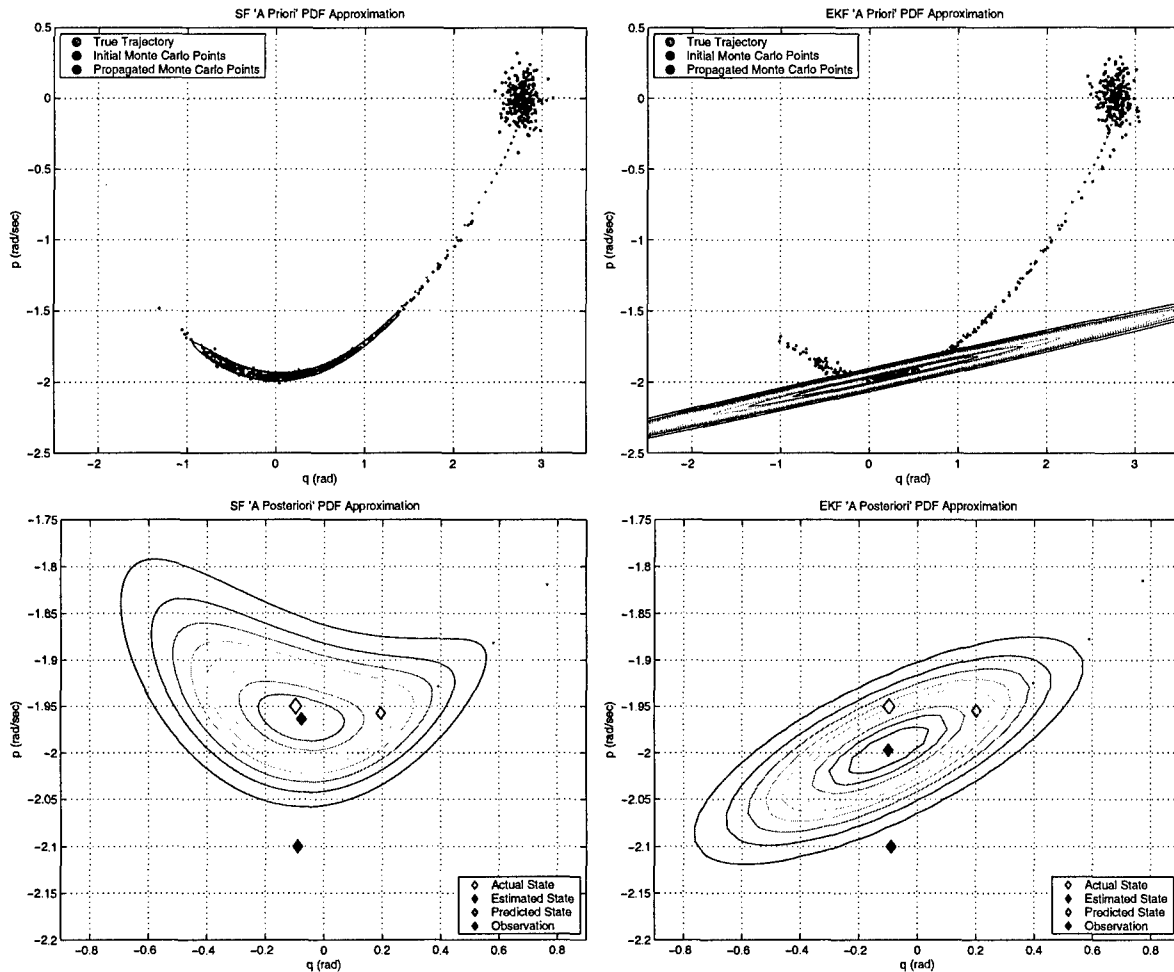


Figure 1. Comparison of SF and EKF PDF Approximations

V. Results

In this section, a number of performance comparisons are made between the SF and the Iterated Extended Kalman Filter (IEKF).² The IEKF is an appropriate benchmark as both the SF and IEKF iteratively solve for the mode of the *a posteriori* pdf as the system's state estimate. The IEKF uses a flight tested, non-symplectic, second-order Adams-Bashforth integrator combined with a non-symplectic second-order state transition matrix algorithm, making it equivalent in numerical order to the propagator and state transition matrix used by the SF. To compare the two estimation methods, realistic satellite configurations and mission profiles were selected for simulation. A representative case is presented here based on the upcoming U.S. Air Force Academy FalconSAT-3 small satellite mission. This is modeled as a 50 kilogram, nearly axisymmetric satellite in a 560 km, moderately inclined, circular orbit with a high-accuracy observation device substituted for the standard low-accuracy magnetometer planned for the actual mission. Instead, the Advanced Stellar Compass (ASC) is modeled due to its successful implementation as a rate-gyro replacement onboard an agile resource-constrained small satellite. It has the ability to provide frequent high-accuracy attitude observations at fast rotation rates. Additionally, it outputs quaternion values, thereby eliminating observation nonlinearity from quaternion-based filters and leaving the dynamical model as the primary source of nonlinearity in the estimation process. For this analysis, ASC sensor noise is modeled as a zero-mean Gaussian white-noise process with the equivalent of one arcsec (1σ) standard deviation in each axis. A symplectic integrator with a small time step relative to the estimation propagators is used to model both the true trajectory and the observation set using the ASC properties outlined above.

For the first simulation, both the SF and the IEKF are limited to one iteration, effectively reducing the IEKF to a standard EKF. Both filters begin with exact knowledge of angular position and rate, and the satellite body begins in a tumbling state with an angular rate vector magnitude of $7^\circ s^{-1}$. For filter initialization, the diagonal values of the covariance matrix for both the IEKF and SF are set to high values relative to the observation noise to ensure initial convergence. Observation noise and process noise are tuned in each filter individually to give optimal performance. A standard small satellite ADCS step size of 0.1 seconds is used for state propagation, and observation frequency is one hertz.

Figure 2 shows the norm of the attitude and rate errors from this simulation. The IEKF attitude estimates converge just below the level of the observation noise. High process noise values relative to observation noise are required to ensure convergence, inhibiting the IEKF's ability to filter out observation noise and more accurately estimate the state. In contrast, the SF attitude estimates converge with a standard deviation that is roughly an order of magnitude below the observation noise standard deviation, demonstrating that the SF is able to improve upon the already high-accuracy observations in this case. Also, the SF norm rate errors are two orders of magnitude less than the IEKF norm rate errors, demonstrating the ability of the SF to provide high-accuracy rate estimation given well-understood dynamics. As expected, the Jacobi-like integral constant is conserved to a high degree of accuracy as well, as seen in figure 3.

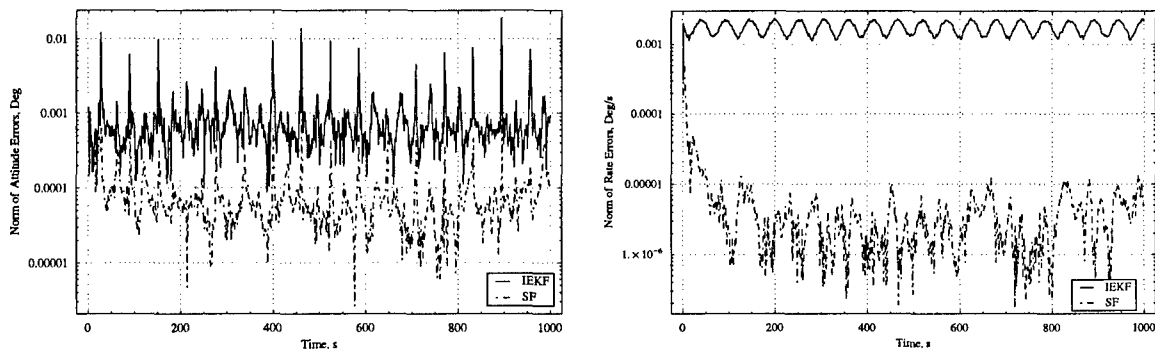


Figure 2. Norm of Attitude and Rate Errors: Single Iteration and No Initial State Errors

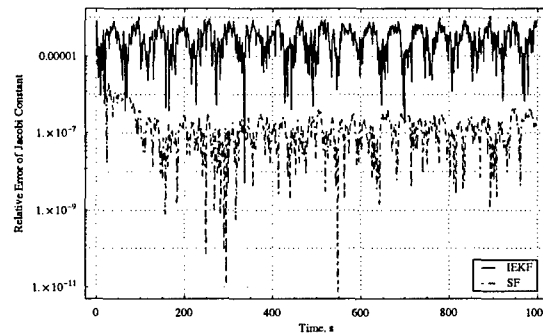


Figure 3. Relative Errors of Jacobi Constant for Simulation 1

To determine the source of the performance difference between the IEKF and the SF, the SF is compared to the symplectic EKF (SKF) in Ref 17. The SF is unique in that it combines a symplectic-preserving dynamical model with a state estimation technique that fully preserves the nonlinear state pdf; in contrast, the SKF combines a symplectic dynamical model with the standard EKF algorithm. Figure 4 illustrates that, given the same initial conditions as the first simulation, the SKF and SF give nearly identical state estimation results. It can be inferred from this equivalence that the symplectic dynamical model is the primary source of performance disparity between the SF and the IEKF observed in figure 2. By using a non-symplectic dynamical model, the IEKF introduces nonlinear errors in state propagation which significantly

impairs its filtering ability. That the model is the main error source is not surprising since the state pdf is unlikely to become significantly nonlinear between the relatively frequent attitude observations modeled in the first simulation. Note that the comparison between the SKF and SF has the additional benefit of validating the SF algorithm by demonstrating its convergence to the Kalman Filter in quasi-linear cases.

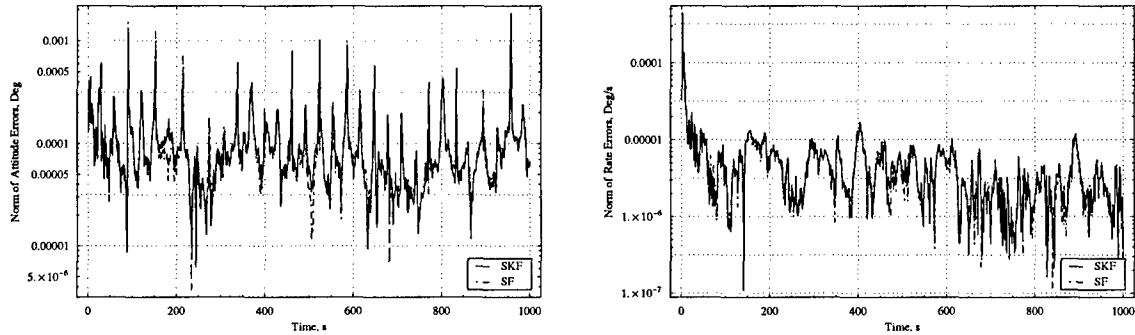


Figure 4. Equivalence of SKF and SF State Estimation

The next simulation demonstrates the strengths of the nonlinear SF state estimate step. In this case, initial attitude errors of 60° , 30° , and 30° in the roll, pitch, and yaw axes, respectively, are combined with initial rate errors of $3^\circ s^{-1}$, $5^\circ s^{-1}$, and $-4^\circ s^{-1}$. Initial attitude covariance is set to $(4^\circ)^2$ in each axis, initial rate covariance is set to $(2^\circ s^{-1})^2$ in each axis, and process noise is equivalent in each filter and low relative to the observation noise. Additionally, observation noise is increased to 100 arcseconds (1σ). This represents a worst-case scenario where the filter is confident in its state estimates though they are significantly biased from the true values. Both filters achieve optimal performance at four iterations per observation, and the results are presented in figures 5 and 6.

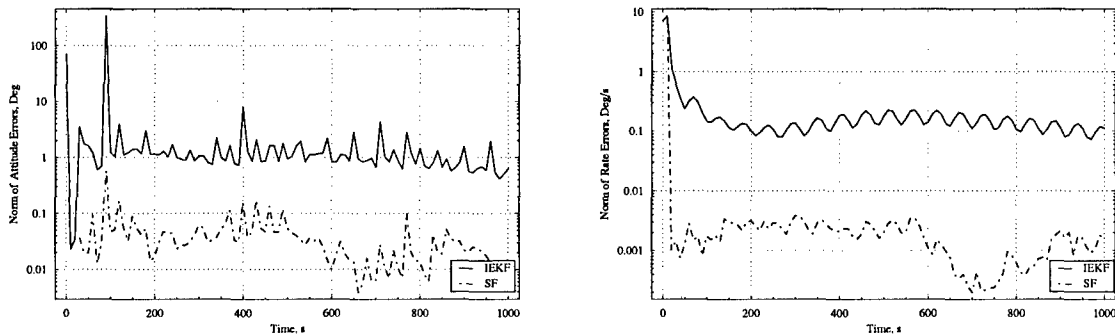


Figure 5. Norm of Attitude and Rate Errors: Multiple Iterations and Large Initial State Errors

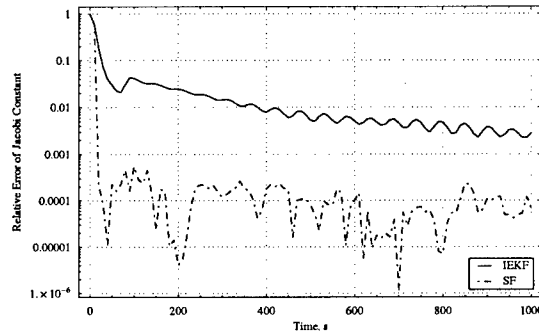


Figure 6. Relative Errors of Jacobi Constant for Simulation 2

In this case, The SF converges much faster than the IEKF to the true state, and its steady-state accuracies are orders of magnitude better than the IEKF's. The higher order moments of the *a posteriori* pdf preserved by the SF state estimation method enable it to more accurately filter observation noise, whereas the IEKF preserves only the first two moments when estimating the state and therefore copes poorly with the nonlinearity induced in the pdf by relatively long spans between observations. By the end of the simulation run presented above, the IEKF has not yet converged to the level of the observation noise. In this case, further iterations of the SF and the IEKF make no appreciable difference in estimation accuracy. Clearly, the SF's symplectic dynamical model and nonlinear state estimation technique enable it to cope with system nonlinearity better than the IEKF.

VI. Conclusions

In this paper a new nonlinear filter for Hamiltonian systems, called the Symplectic Filter, has been presented. It is unique in that it combines a symplectic dynamical model with a nonlinear estimation process that fully preserves the probability density function when determining the system state. It is also computationally efficient as it propagates error covariances using Extended Kalman Filter equations which have been modified to preserve the underlying geometry of Hamiltonian systems. By combining a theoretically correct approach to state estimation with efficient recursion methods, the Symplectic Filter aims to provide accurate estimation for small satellites with limited computational resources.

Comparisons with a non-symplectic second-order Iterated Extended Kalman Filter demonstrate the strengths of the SF when applied to the satellite attitude problem. In the first case, the symplectic dynamical model of the SF enables it to reduce frequent high-accuracy attitude observation errors by an order of magnitude while the IEKF is only able to converge to the observation noise. In the second case, the nonlinear state estimation method of the SF enables it to converge to the true solution with a high degree of accuracy given large initialization errors. These results demonstrate the merit of the nonlinear Symplectic Filter and its suitability for use onboard agile small satellites that require high accuracy, computationally efficient attitude estimation methods.

Acknowledgments

The authors would like to thank the Marshall Aid Commemoration Commission for its generous support via the Marshall Scholarship, and acknowledge the Surrey Space Centre Astrodynamics Group, and in particular David Wokes, for technical assistance throughout the research effort.

References

- ¹Athans, M., Wishner, R. P., and Bertolini, A., "Suboptimal State Estimation for Continuous-Time Nonlinear Systems from Discrete Noisy Measurements," *IEEE Transactions on Automatic Control*, Vol. AC-13, No. 5, 1968, pp. 504–514.
- ²Jazwinski, A. H., *Stochastic Processes and Filtering Theory*, Vol. 64 of *Mathematics in Science and Engineering*, Acad-

emic Press, London, 1st ed., 1970.

³Kushner, H. J., "Nonlinear Filtering: The Exact Dynamical Equations Satisfied by the Conditional Mode," *IEEE Transactions on Automatic Control*, Vol. AC-12, No. 3, 1967, pp. 262-267.

⁴Bellaire, R. L., *Nonlinear Estimation with Applications to Target Tracking*, Ph.D. thesis, Georgia Institute of Technology, 1996.

⁵Haykin, S. and Freitas, N. D., "Special Issue on Sequential State Estimation," *Proceedings of the IEEE*, Vol. 92, No. 3, 2004, pp. 399-400.

⁶Julier, S., Uhlmann, J., and Durrant-Whyte, H. F., "A New Method for the Nonlinear Transformation of Means and Covariances in Filters and Estimators," *IEEE Transactions on Automatic Control*, Vol. 45, No. 3, 2000, pp. 477-482.

⁷Gelb, A., editor, *Applied Optimal Estimation*, The M.I.T. Press, Cambridge, MA, 1974.

⁸Brown, R. G. and Hwang, P. Y. C., *Introduction to Random Signals and Applied Kalman Filtering*, John Wiley & Sons, New York, 3rd ed., 1997.

⁹Vallado, D. A., *Fundamentals of Astrodynamics and Applications*, Microcosm Press, London, 2nd ed., 2001.

¹⁰Palmer, P., Mikkola, S., and Hashida, Y., "A Simple High Accuracy Integrator for Spacecraft Attitude Systems," *AIAA Guidance, Navigation, and Control Conference*, Providence, Rhode Island, 2004.

¹¹Arulampalam, M. S., Maskell, S., Gordon, N., and Clapp, T., "A Tutorial on Particle Filters for Online Nonlinear/Non-Gaussian Bayesian Tracking," *IEEE Transactions on Signal Processing*, Vol. 50, No. 2, 2002, pp. 174-188.

¹²Challa, S. and Bar-Shalom, Y., "Nonlinear Filter Design Using Fokker-Planck-Kolmogorov Probability Density Evolutions," *IEEE Transactions on Aerospace and Electronic Systems*, Vol. 36, No. 1, 2000, pp. 309-315.

¹³Vathsal, S., "Spacecraft Attitude Determination Using a Second-Order Nonlinear Filter," *Journal of Guidance, Control, and Dynamics*, Vol. 10, No. 6, 1987, pp. 559-566.

¹⁴Lappas, V. J., Steyn, W. H., and Underwood, C. I., "Experimental Testing of a CMG Cluster for Agile Microsatellites," *IEEE 11th Mediterranean Conference on Control and Automation*, Rhodes, Greece, 2003.

¹⁵Mikkola, S., Palmer, P., and Hashida, Y., "A Symplectic Orbital Estimator for Direct Tracking on Satellites," *Journal of Astronautical Sciences*, Vol. 48, No. 1, 1999, pp. 109-125.

¹⁶Imre, E. and Palmer, P., "A Numerical Approach to High Precision Numerical Relative Orbit Propagation," *AAS/AIAA Astrodynamics Specialist Conference*, Lake Tahoe, California, 2005.

¹⁷Valpiani, J. and Palmer, P., "Symplectic Attitude Estimation for Small Satellites," *AAS/AIAA Space Flight Mechanics Meeting*, Tampa, Florida, 2006.

¹⁸Sanyal, A., Lee, T., Leok, M., and McClamroch, N. H., "Global Optimal Attitude Estimation using Uncertainty Ellipsoids," *Systems And Control Letters*, submitted for publication, 2006.

¹⁹Lee, T., Sanyal, A., Leok, M., and McClamroch, N. H., "Deterministic Global Attitude Estimation," *IEEE Conference on Decision and Control*, submitted for publication, San Diego, California, 2006.

²⁰Touma, J. and Wisdom, J., "Lie-Poisson Integrators for Rigid Body Dynamics in the Solar System," *The Astronomical Journal*, Vol. 107, No. 3, 1994, pp. 1190-1202.

²¹Park, R. S. and Scheeres, D. J., "Nonlinear Mapping of Gaussian State Uncertainties: Theory and Applications to Spacecraft Control and Navigation," *AAS/AIAA Astrodynamics Specialists Conference*, Lake Tahoe, CA, 2005.

²²Shivarama, R. and Fahrenthold, E. P., "Hamilton's Equations with Euler Parameters for Rigid Body Modeling," *ASME Journal of Dynamic Systems, Measurement, and Control*, Vol. 126, 2004, pp. 124-130.

²³Hall, C. D. and Beck, J. A., "Relative Equilibria of Orbiting Gyrostats," *AAS/AIAA Astrodynamics Specialist Conference*, Girdwood, Arkansas, 1999.

²⁴Wang, L.-S. and Krishnaprasad, P. S., "Hamiltonian Dynamics of a Rigid Body in a Central Gravitational Field," *Celestial Mechanics and Dynamical Astronomy*, Vol. 50, 1991, pp. 349-386.

²⁵Hayes, W., *A Brief Survey of Issues Relating to the Reliability of Simulation of the Large Gravitational N-body Problem*, Ph.D. thesis, University of Toronto, 1996.

²⁶Leimkuhler, B. and Reich, S., *Simulating Hamiltonian Dynamics*, Cambridge Monographs on Applied and Computational Mathematics, Cambridge University Press, Cambridge, 2004.

²⁷Arnold, V. I., *Mathematical Models of Classical Methods*, Graduate Texts in Mathematics, Springer, London, 2nd ed., 1974.

²⁸Wertz, J. R., editor, *Spacecraft Attitude Determination and Control*, Kluwer Academic Publishers, London, 1978.

²⁹Hall, C. D., "When Spacecraft Won't Point," *Advances in Astronautical Sciences*, Vol. 116, 2004, pp. 79-86.

³⁰Jorgensen, J. L., Denver, T., Betto, M., and den Braembussche, P. V., "The PROBA Satellite Star Tracker Performance," *4th IAA Symposium on Small Satellites for Earth Observation*, Berlin, Germany, 2003.

³¹Bell, B. M. and Cathey, F. W., "The Iterated Kalman Filter Update as a Gauss-Newton Method," *IEEE Transactions on Automatic Control*, Vol. 38, No. 2, 1993, pp. 294-297.

³²Crassidis, J. L. and Markley, F. L., "Unscented Filtering for Spacecraft Attitude Estimation," *Journal of Guidance, Control, and Dynamics*, Vol. 26, No. 4, 2003, pp. 536-542.

³³Press, W. H., Teukolsky, S. A., Vetterling, W. T., and Flannery, B. P., *Numerical Recipes in C*, Cambridge University Press, Cambridge, 2nd ed., 1992.

³⁴Vaisman, I., "Lectures on the Geometry of Poisson Manifolds," *Bulletin of the American Mathematical Society*, Vol. 33, No. 2, 1996, pp. 255-261.